

This is an electronic reprint of the original article. This reprint may differ from the original in pagination and typographic detail.

Implementation of Experimental Design Techniques to Optimize Immunoglobulins Detection with Ultrasensitive Sandwich Immunoassays

Scandurra, Cecilia; Bollella, Paolo; Österbacka, Ronald; Leonetti, Francesco; Macchia, eleonora; Torsi, L.

Published in:
Advanced Sensor Research

DOI:
[10.1002/adsr.202200009](https://doi.org/10.1002/adsr.202200009)

Published: 25/12/2022

Document Version
Final published version

Document License
CC BY

[Link to publication](#)

Please cite the original version:

Scandurra, C., Bollella, P., Österbacka, R., Leonetti, F., Macchia, E., & Torsi, L. (2022). Implementation of Experimental Design Techniques to Optimize Immunoglobulins Detection with Ultrasensitive Sandwich Immunoassays. *Advanced Sensor Research*, 1(1), Article 202200009. <https://doi.org/10.1002/adsr.202200009>

General rights

Copyright and moral rights for the publications made accessible in the public portal are retained by the authors and/or other copyright owners and it is a condition of accessing publications that users recognise and abide by the legal requirements associated with these rights.

Take down policy

If you believe that this document breaches copyright please contact us providing details, and we will remove access to the work immediately and investigate your claim.

Implementation of Experimental Design Techniques to Optimize Immunoglobulins Detection with Ultrasensitive Sandwich Immunoassays

Cecilia Scandurra, Paolo Bollella, Ronald Österbacka, Francesco Leonetti, Eleonora Macchia,* and Luisa Torsi

The ultrasensitive measurement of protein markers plays a pivotal role in the early diagnosis of infectious and progressive diseases. Recently, digital methods such as those enabled by the Simoa Planar Array technology (SP-X System) have made significant progress in reaching ultrasensitive detection with clinically relevant protein biomarkers. The elicited Simoa technology is based on printing high-density capturing antibodies layers on the bottom of the wells of a microtiter plate, followed by a standard sandwich-type immunometric chemiluminescent detection. Such assay, reaching limit-of-detections (LODs) in the low femtomolar range, can be conveniently customized. An optimized Simoa SP-X assay for detecting and quantifying immunoglobulin M (IgM, non-specific indicator of inflammation) is developed herein and optimized. A full factorial experimental design is undertaken to optimize the assay, leading to a reduced experimental effort and increased quality of the information obtained concerning the traditional one-variable-at-a-time approach. The optimization process leads to an IgM LOD of 4 fM that compares well with those achieved with commercially available Simoa Planar Array kits. Remarkably, depositing both the capturing and detecting layer from a solution ($0.1 \mu\text{g mL}^{-1}$) one order of magnitude less concentrated than in standard kits is needed, and the assay's cost is sizably reduced.

1. Introduction

Identifying proteins, peptides, and genetic markers with femtomolar detection limits have been recently considered a fundamental task to enable early diagnostics. Indeed, the possibility to detect clinically relevant biomarkers at very low concentrations might allow a better understanding of the etiology of many illnesses states and enable early diagnosis of progressive and infectious diseases.^[1–4] Consequently, it is of paramount importance to endow clinicians with powerful analytical tools for the accurate and sensitive detection of biomarkers. Although standard medical analysis usually foresees nucleic acids or proteins and peptides as biomarkers,^[5] genetic ones, such as DNA or RNA strands, are most often employed in a wide range of clinical applications.^[6] Indeed, the use of genetic biomarkers for clinical purposes can be dated back to 1999^[7] to differentiate among two different forms of leukemia and later, has been employed to identify oncogenes alterations through a wide variety of different

genomic markers.^[8–10] Next-Generation Sequencing (NGS) technique, being the most sensitive approach to genetic markers with a limit of detection (LOD) of one single DNA or RNA copy,^[11] has a significant advancement in the identification of genetic markers for early detection of progressive diseases. On the other hand, a pivotal role in the early diagnosis of many pathological states is also played by peptide and protein biomarkers.^[12] Consequently, a huge effort has been dedicated to ultrasensitive proteins detection.^[13–16] However, ultrasensitive protein detection remains an extremely challenging task.


Recently, the Simoa Planar Array technology (SP-X System)^[17] has been developed based on a multiplex ELISA system encompassing digital chemiluminescent imaging of an array of capture antibodies.^[18,19] The Simoa SP-X technology can sense proteins markers with LODs in the femtomolar (10^{-15} M) range, corresponding to 10^5 – 10^6 proteins in a sample volume of 100 μL , hence being sensitive to a far less extent than NGS. Such femtomolar sensitivity relies on printing arrays of

C. Scandurra, P. Bollella, L. Torsi
Dipartimento di Chimica
Università degli Studi di Bari "Aldo Moro"
Bari 70125, Italy

P. Bollella, E. Macchia, L. Torsi
CSGI (Centre for Colloid and Surface Science)
Bari 70125, Italy
E-mail: eleonora.macchia@uniba.it

R. Österbacka, E. Macchia, L. Torsi
The Faculty of Science and Engineering
Åbo Akademi University
Turku 20500, Finland

F. Leonetti, E. Macchia
Dipartimento di Farmacia-Scienze del Farmaco
Università degli Studi di Bari "Aldo Moro"
Bari 70125, Italy

 The ORCID identification number(s) for the author(s) of this article can be found under <https://doi.org/10.1002/adsr.202200009>

DOI: 10.1002/adsr.202200009

highly packed antibodies onto detection spots holding an area of 0.13 mm^2 .^[20–22]

The user-customizable Simoa SP-X Homebrew assays, combining contact printing technology with anchor antibody/peptide tag pairs, have recently been demonstrated^[23] to detect different analytes for specific requirements with femtomolar sensitivities. However, each specific application's consistency and assay performance need to be assessed, typically encompassing the optimization of many experimental parameters, such as the concentrations of capture and detection antibodies involved in the sandwich immunoassay. In this study, a full factorial experimental design approach has been undertaken to optimize the sensitivity of a Simoa SP-X Homebrew assay to detect and quantify IgM, a non-specific indicator of inflammation, used as a prototype system. Indeed, factorial experimental design techniques are beneficial for determining essential parameters and their effects on the assay while minimizing the number of experiments.^[24,25] The experimental design represents an extremely powerful tool when optimizing assays encompassing many parameters, offering many advantages concerning the traditional one-variable-at-time (OVAT) approaches. Indeed, to the best of our knowledge experimental design has never been proposed to optimize Single molecule array (Simoa) assays. Indeed, currently the development and optimization of Simoa SP-X assays is performed with a OVAT approach.^[21] Moreover, only one study reports an optimization of a sandwich ELISA assay based on a Plackett–Burnman screening design aiming at determine the best enzyme label as well as the substrate incubation time.^[26] Instead, the goal of our study is to develop for the first time an assay for IgM prototype system minimizing the reagent consumption of the final assay, using a model based on a full factorial 2^2 experimental design. Remarkably, the experimental design approach herein provided rather detailed knowledge of the impact of the concentrations of the capture and detection antibodies on the assay sensitivity in the whole experimental domain. To this end, the experimental design has been used to detect the minimum set of experiments resulting in the highest possible information in any point of the experimental domain, which has been predicted using a 2^2 factorial model. Moreover, such approach allowed to elucidate and taking into account the main trends and interactions among the capture and detection antibodies concentrations involved in the assay. The proposed model has been validated, showing an excellent prediction capability and settling the assay conditions that minimized the LOD of the IgM assays. Remarkably, a LOD as low as 4 fM has been achieved with minimum capture and detection antibodies consumption. Indeed, the LOD herein demonstrated with polyclonal anti-IgM capture and detection antibodies well compared with the LODs typically achieved with commercially available Simoa SP-X kits^[17,19] reducing the involved antibodies concentrations by one order of magnitude and hence dramatically reducing the costs of the assay. Therefore, the novelty of this study relies on the use of a model based on a full factorial design to develop for the first time a customizable Simoa immunoassay, where IgM has been used as a prototype system. Remarkably, given the general approach involved in the optimization of the assay, this multivariate optimization process is in principle applicable to different sandwich immunoassays with a wide spectrum of bio-markers.

2. Results and Discussion

2.1. Results

The main steps of the IgM Simoa SP-X assay are given in **Figure 1**. The assay encompasses a 96-well ELISA plate, shown in **Figure 1a**, hosting 12 distinct circular spots, $600 \mu\text{m}$ in diameter, in each well, as shown in **Figure 1b**.^[17] The anti-IgM peptide-tagged capture antibodies first bind the plate-bound anchor antibody deposited in the first place of each well. Then the assay workflow, schematically depicted in **Figure 1c**, proceeds as customary for sandwich immunoassay format: the analyte is sandwiched between the peptide-tagged capture and biotinylated detector antibodies. In particular, each IgM standard solution, with concentrations ranging from 2.5 pg mL^{-1} (2.5 fM) to 10 ng mL^{-1} (10 pM), was incubated in each well, and the microtiter plate was shaken at a controlled temperature. The target analyte was captured at the specific spot hosting the anti-IgM capture antibodies. Then, the microtiter plate was washed thoroughly and incubated with the anti-IgM detection antibodies labeled with biotin, forming sandwich immunocomplexes with the capture antibody–antigen complexes. Afterward, the plate was washed to remove unreacted antibodies and incubated with SA-HRP to label the immunocomplexes with enzymes. Eventually, luminol and H_2O_2 were incubated in each well. Consequently, the enzyme–substrate reaction yielded light emitted locally from the immunocomplexes. The intensity of the signal is directly proportional to the concentration of analyte in the analyzed solution and imaged on a charge-coupled device (CCD) camera.

The sensitivity of the Simoa SP-X homebrew assay with the IgM/anti-IgM prototype system has been optimized through an experimental design approach, encompassing two factors: the concentration of the anti-IgM capture antibody and the concentration of the detection antibody. The typical experimental setting for capturing and detecting antibodies' concentrations used in the sandwich immunoassay system has been used as a starting point.^[16,27,28]

In particular, the explored experimental domain encompasses anti-IgM capture and detection antibodies' concentrations ranging from 1 to $50 \mu\text{g mL}^{-1}$ as starting point, based on the antibodies concentrations typically employed in immunoassay development.^[17,27,29,30] Following a two-level design, those two quantitative variables have been coded as X_1 and X_2 , representing the capture and detection antibodies concentration respectively, settled at low and high level, namely -1 and $+1$. The graphical representation of the experimental domain explored by the 2^2 factorial design is schematically depicted in **Figure 2a**.

From a geometrical point of view, the 2^2 factorial design explores the corner of a square, meaning that, unlike in the OVAT, in which variable X_1 is changed while variable X_2 is kept constant, the model herein developed allows both variables to change simultaneously. The output of the experiment performed at the corners of the experimental domain, marked by the black points (in **Figure 2a**, has been used to feed the model. In addition, two experiments have been performed at the center point, shown as a red dot in **Figure 2a**, have been used to assess the model's prediction capability. The experimental matrix and the experimental plan have been summarized in **Table 1**. It is worth mentioning

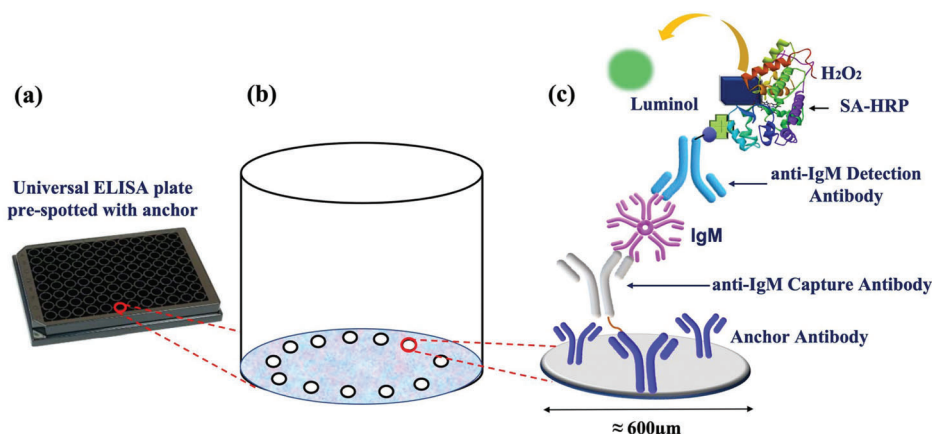


Figure 1. a) Picture of the 96-well ELISA plate pre-spotted with the anchor antibody. b) Schematic representation of the single well with 12 distinct spots, where the first spot highlighted in red is covered with highly packed printed anchor antibodies, holding a high affinity for the peptide tag. c) Workflow of the Simoa Homebrew assay developed for detection of IgM target molecule.

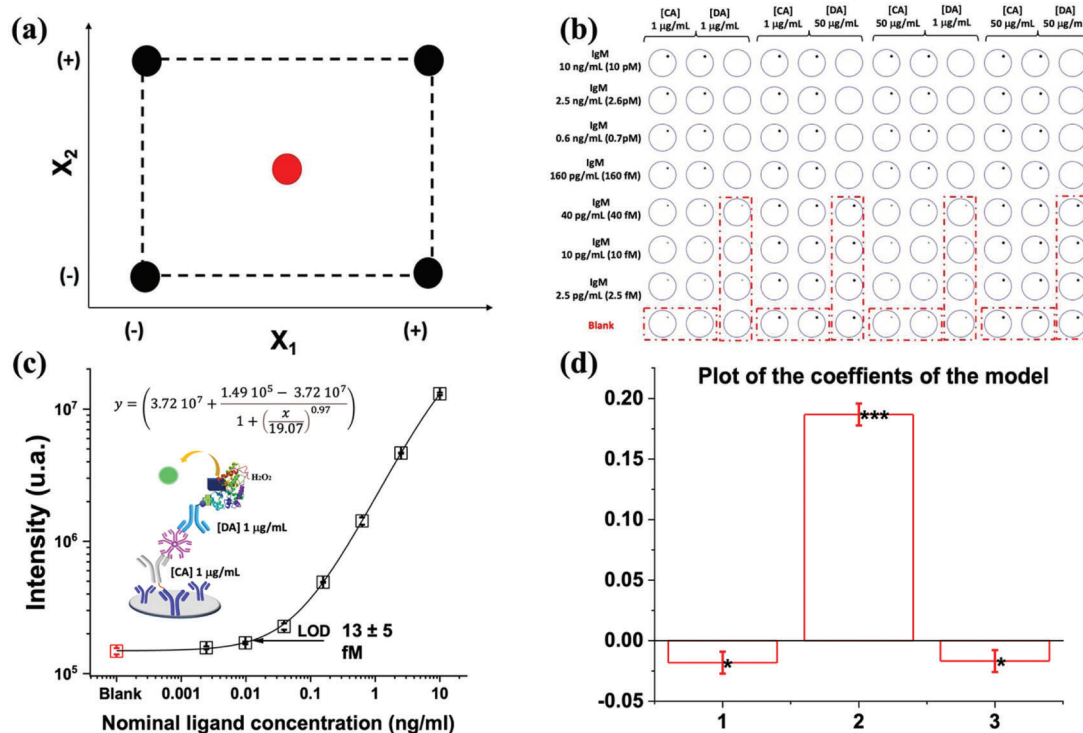


Figure 2. a) Graphical representation of the 2^2 factorial design. b) Simoa SP-X assay layout used to develop the model along with the microtiter plates read on the SP-X imager (Quanterix Corporation) by the CCD camera. c) Calibration curve for IgM registered with $1 \mu\text{g mL}^{-1}$ of capture and detection anti-IgG antibodies. Error bars are shown for two replicate measurements of IgM sensing (black squares) and six replicate measurements of blank (red square). d) Graphical representation of the coefficients of the model of the LOD of 2^2 factorial design. The error bars are the confidence level at $p = 0.05$, while the stars indicate the significance of the coefficients (* = $p < 0.05$, ** = $p < 0.01$, *** = $p < 0.001$).

that, while the experimental matrix contains the coded values of variables X_1 and X_2 , namely -1 and $+1$, the experimental plan reports the real values of the concentrations of the capture ([CA]) and detection ([DA]) antibodies expressed in $\mu\text{g mL}^{-1}$.

As apparent from the experimental plan in Table 1, six Simoa SP-X assays have been conducted under different conditions, namely using concentrations of $1 \mu\text{g mL}^{-1}$ for both capture and detection antibodies as triplicate, $50 \mu\text{g mL}^{-1}$ of capture antibody

and $1 \mu\text{g mL}^{-1}$ of detection antibody and vice versa, and finally $50 \mu\text{g mL}^{-1}$ for both antibodies. Since the following mathematical model has been foreseen

$$Y = b_0 + b_1 X_1 + b_2 X_2 + b_{12} X_1 X_2 \quad (1)$$

four assays are necessary to estimate the constant term, two linear terms, and one two-term interaction while having two degrees

Table 1. Experimental matrix, experimental plan, and responses of the 2² Full Factorial Design, along with the center point used for the model validation.

X ₁	X ₂	[CA] [μg mL ⁻¹]	[DA] [μg mL ⁻¹]	LOD [ng mL ⁻¹]	LOD [fM]
-1	-1	1	1	0.01	10
-1	-1	1	1	0.01	10
-1	-1	1	1	0.02	18
+1	-1	50	1	0.01	10
-1	+1	1	50	0.42	442
+1	+1	50	50	0.35	368
0	0	25	25	0.22	229
0	0	25	25	0.17	180

of freedom left to define the statistical significance of the model coefficients. Indeed, by computing the four coefficients from only four experiments, and therefore having no degrees of freedom available, it would be not possible to estimate the experimental variability, thus hindering the evaluation of a statistical significance of the coefficients. Therefore, the assay encompassing a concentration of 1 μg mL⁻¹ for both capture and detection antibodies has been performed in triplicate, allowing to perform the diagnostic of the model proposed in this study. The selected design gives maximum leverage of 1 only for a small part of the experimental domain, while for most of the domains the leverage is lower, with the average leverage of 0.33. Indeed, the leverage has been computed in the whole experimental domain, based on the experimental matrix and the postulated model. Importantly the leverage, multiplied by the experimental variance, corresponds to the variance of the estimated response at that point.^[31] Therefore, a leverage of 1 means that the model will predict the response with the same precision of the experiment, while a leverage <1 means that the response can be predicted with better precision than the experimental data collected under the same conditions. Consequently, it is possible to infer that the model holds an excellent predictive ability, i.e., a leverage <1, in most of the experimental domains. The Simoa SP-X assays' layout has been shown in Figure 2b, along with the CCD image map collected with SP-X imager. For each assay, the dose–response curves have been registered in duplicate, incubating the first seven rows of the microtiter plate with IgM standard solutions spanning the whole dynamic range of the assay. The 8th row of the assay has been used to measure the blank signal. Four additional wells for each assay, highlighted with red dashed lines in Figure 2b, have been used to register the blank signal, resulting in six replicates of the noise level. The dose–response curves registered for the assay encompassing a concentration of 1 μg mL⁻¹ for both the capture and detection antibodies are shown in Figure 2c. The black squares are relevant to the average of the exposure to IgM analyte standard solutions evaluated with two replicates, while the red square is the average of the signal of the blanks over six replicated experiments. The black line represents the curve fit, being a 5-Parameter Logistic (5PL) based on the following Equation:

$$I = a + \frac{d}{\left(1 + \left(\frac{x}{c}\right)^b\right)^e} \quad (2)$$

where x is the IgM concentration, while I is the CCD image intensity, expressed in arbitrary units. The parameters a and d represent the minimum and maximum response of the curve, b is defined as the Hill Coefficient, c is the inflection point where the curvature changes signs, and e is the non-symmetry term. The fitting procedure has been repeated several times, and the coefficients have been adjusted depending on the residual errors in the previous iteration. The LOD of each assay, taken as the response of the 2² factorial design, has been computed as the concentration providing a response equal to

$$I_{\text{blank}} \pm k\sigma \quad (3)$$

where I_{blank} is the average CCD image intensity of the noise level of the six blank data plus three times (k) the standard deviation of the noise (σ).^[12,32] Indeed, IUPAC recommends a value of $k = 3$ as the probability of a blank signal being threefold higher than the I_{blank} (i.e., a false positive) is <1 %. The LOD levels for each IgM assay performed at the corner of the experimental domain have been evaluated according to Equation 3, while the curve fit according to Equation 2 enables to correlate this value to the concentration of the LOD. An average LOD of (13 ± 5) fM (13 ± 5 pg mL⁻¹) has been evaluated for the triplicate assay conducted with a 1 μg mL⁻¹ concentration for both the capture and detection antibodies. The LOD increases to 442 ± 20 fM (0.42 ± 0.02 ng mL⁻¹) when the detection antibody concentration increases to 50 μg mL⁻¹, showing that the detection antibody concentration plays a critical role in optimizing the sensitivity of the sandwich assay. The error bar has been taken as the pooled standard deviation evaluated in the experimental domain. Indeed, as it is apparent from the CCD image intensity reported in Figure 2b, by increasing the detection antibody concentration from 1 to 50 μg mL⁻¹, the blank signal increases by ≈30%, resulting in a lower sensitivity of the assay. Indeed, the higher blank signal can be ascribed to possible interactions of the detection antibodies with unreacted anchor antibodies, introducing spurious background signals. Indeed, to achieve low assay backgrounds, or in other words, low noise, it is important to prevent the non-specific binding of non-target molecule components of the assay.^[17]

The multilinear regression coefficients of the model reported in Equation 2 have been determined along with their significance to elucidate the effect of the capture and detection antibodies concentrations, as shown in Figure 2d.

The analysis provided the following model:

$$Y(\text{LOD}) = 0.19 - 0.018X_1^{(*)} + 0.18X_2^{(*)} - 0.016X_1X_2^{(***)} \quad (4)$$

where the significance level is indicated according to the usual convention: * $p < 0.05$, ** $p < 0.01$, *** $p < 0.001$. The terms of the model are all significant terms, although the linear terms of X_2 hold an absolute value larger than the other ones. The large coefficient of X_2 indicates that by increasing the concentration of the detection antibody, an increase in the LOD of the assay is registered, and therefore better results are obtained by reducing this concentration. Moreover, the coefficient of the linear term of X_1 is negative, and since the LOD has to be minimized, it can be said that the assay's sensitivity improves working with a higher concentration of capturing antibodies. However, since the coefficient for each term represents the change in the mean response

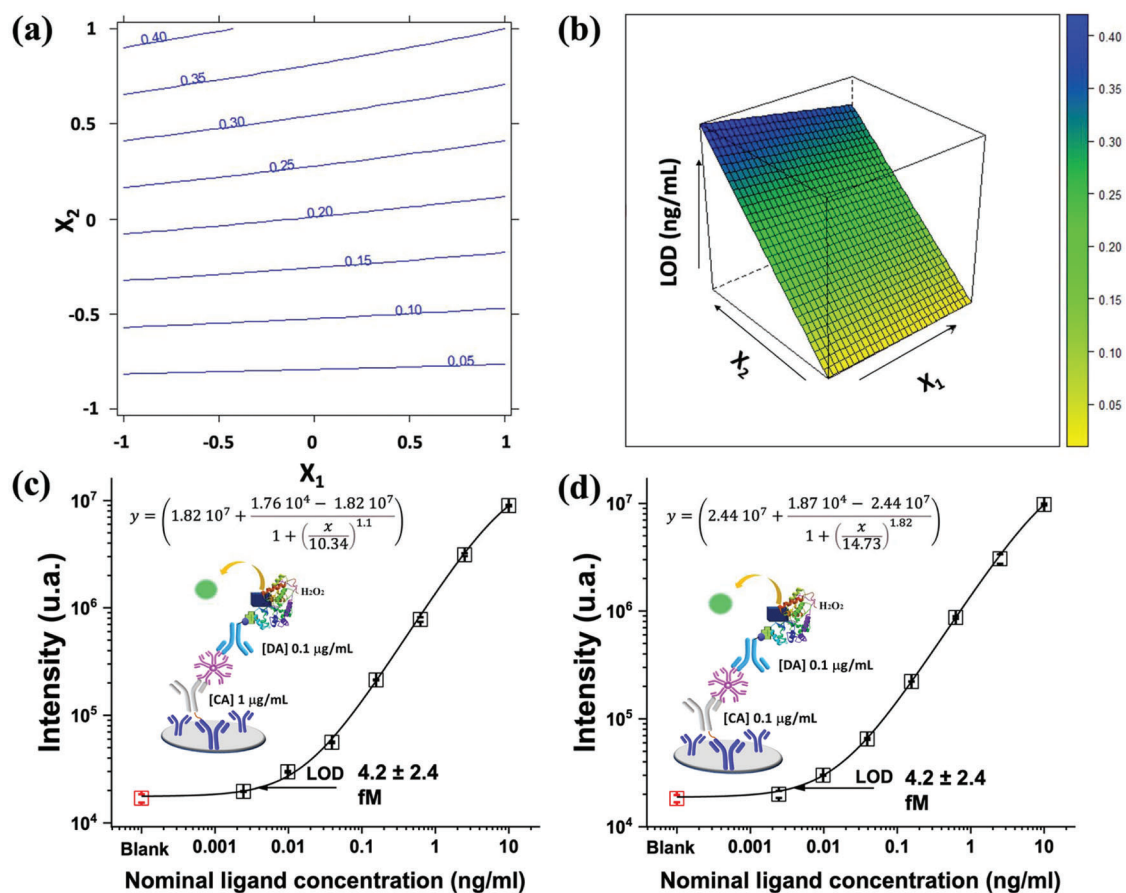


Figure 3. a) Isoresponse contour plot of the LOD response of the 2^2 factorial design along with b) the Response Surface. c) Calibration curve for IgM registered with $1 \mu\text{g mL}^{-1}$ of capture antibodies and $0.1 \mu\text{g mL}^{-1}$ of detection antibodies. d) Calibration curve for IgM registered with $0.1 \mu\text{g mL}^{-1}$ of both capture and detection anti-IgM antibodies. Error bars are shown for two replicate measurements of IgM sensing (black squares) and six replicate measurements of blank (red square).

associated with an increase of one coded unit in that term, while the other terms are kept constant, it can be noted that by increasing the capture antibody concentration from 1 to $50 \mu\text{g mL}^{-1}$, the decreases registered in the LOD = 18 fM.

As far as concerns X_1 and X_2 , as their interaction is significant, it is impossible to interpret their effect by taking into account their coefficients in the model. Instead, the isoresponse plot will be analyzed in the following (Figure 3a, vide infra). To validate the model, the predicted response at the center point, namely the assay performed with $25 \mu\text{g mL}^{-1}$ for both concentrations of the capture and detection antibodies, has been compared with the experimental value. The predicted LOD value in the center point is 190 fM (0.19 ng mL^{-1}). The experimental values of the two replicates are 229 fM (0.22 ng mL^{-1}) and 180 fM (0.17 ng mL^{-1}), and therefore the average value is 194 fM (0.19 ng mL^{-1}). The experimental pooled standard deviation is 20 fM (0.02 ng mL^{-1}), with four degrees of freedom. The semi-amplitude of the confidence interval of the mean can be computed as $t \cdot \sigma / \sqrt{N}$, where t is the critical t -student value with a confidence level of 0.05 and 4 degrees of freedom, and N is the number of replicates that have been performed. Therefore, the experimental value at the center point is $(194 \pm 30) \text{ fM}$, corre-

sponding to $0.19 \pm 0.03 \text{ ng mL}^{-1}$, which is not significantly different from the predicted value (190 fM, 0.19 ng mL^{-1}). Thus, the model is validated and accepted in the whole experimental domain.

2.2. Discussion

The isoresponse contour plot, reported in Figure 3a, provides important information about the interactions among the two variables X_1 and X_2 .

Indeed, the geometrical shape of a linear model without interactions is a plane, leading to isoresponse lines that are parallel, while if relevant interactions are present, the contour plot shows a distorted plane with the isoresponse lines not parallel. From the isoresponse plot shown in Figure 3a, it can be seen that at a higher concentration of detection antibody, the effect of increasing the capture antibody concentration is more relevant. In comparison, at lower detection antibody concentration, the capture antibody concentration has no effect. Moreover, the response surface in Figure 3b clearly shows that the best condition in the explored experimental domain corresponds to a lower

detection antibody concentration. On the other hand, an increase in the capture antibody concentration is not producing an essential improvement in the sensitivity while dramatically impacting the cost of the reagents of the assay. As a further step, the concentrations of capture and detection antibodies have been further reduced outside the experimental domain to enhance the assay sensitivity while minimizing the cost of the assay. In Figure 3c, the calibration curve registered for IgM assay encompassing $1 \mu\text{g mL}^{-1}$ of capture antibodies and $0.1 \mu\text{g mL}^{-1}$ of detection antibodies is reported.

A decrease in the blank signal of $\approx 20\%$ has been registered with respect to the assay performed with a $1 \mu\text{g mL}^{-1}$ concentration for both capture and detection antibodies. Moreover, a LOD as low as $(4.2 \pm 2.4) \text{ fM}$ ($4.2 \pm 2.4 \text{ pg mL}^{-1}$) has been achieved, $\approx 70\%$ lower than the LOD registered with the assay encompassing a concentration of $1 \mu\text{g mL}^{-1}$ for both the capture and detection antibodies. Therefore, the reduction of the detection antibody concentration at $0.1 \mu\text{g mL}^{-1}$ allowed to improve the signal-to-background ratio and thus further improve the sensitivity of the assay. The effect of a reduction of capture antibody concentration has been investigated too. Indeed, the Simoa SP-X assay encompassing a concentration of $0.1 \mu\text{g mL}^{-1}$ for both the capture and detection antibodies, shown in Figure 3d, produced comparable results in terms of signal-to-background ratio and LOD with the assay reported in Figure 3c. In other words, reducing the capture antibody concentration by one order of magnitude has not significantly affected the Simoa SP-X assay. Such an occurrence can be explained considering that an anti-IgM footprint occupies a surface of $\approx 300 \text{ nm}^2$,^[33] and thus $\approx 10^9$ anti-IgM can be hosted on the $600 \mu\text{m}^2$ pre-spotted area of the microtiter plate wells. The anti-IgM is thus packed on the spot of the Simoa SP-X plate at a density of $10^3 \mu\text{m}^{-2}$, being comparable to the density of bioreceptors on the large-area detecting interface of ultrasensitive biosensing platforms currently available.^[14] Considering an incubation volume of $50 \mu\text{L}$ for the capture antibody solution, a minimum concentration of 30 pM , corresponding to 4.5 ng mL^{-1} , is necessary to cover the Simoa SP-X spot fully. Indeed, an IgM assay encompassing a concentration of 1 ng mL^{-1} (7 pM) of capture antibody, slightly below the minimum concentration necessary to saturate the detecting spot area, while keeping fixed at $0.1 \mu\text{g mL}^{-1}$ the detection antibody concentration, has been performed, recording a signal falling into the background level.

3. Conclusion

Full factorial experimental design techniques were successfully used to elucidate the effects of the concentrations of capture and detection anti-IgM antibodies on the sensitivity of a Simoa SP-X assay to detect IgM marker, used as a prototype system. The proposed model provided an indication of the parameters' values where the optimal conditions in terms of sensitivity may be found. As the optimization of sandwich immunoassay typically involves using multiple parameters, the experimental design techniques are proposed in this study as part of the experimental strategy to deploy and optimize Simoa SP-X homebrew assays for many clinical applications. Remarkably, a LOD as low as 4 fM has been demonstrated with polyclonal anti-IgM capture and detection antibodies, reducing the involved antibody concentrations by one order of magnitude. Such LOD value, registered

with a cost-effective assay, well compares with the LODs typically achieved with commercially available Simoa SP-X kits.

4. Experimental Section

Materials: Anti-human immunoglobulin M (anti-IgM) polyclonal antibodies produced in goat and human IgM (Molecular weight $M_w \approx 950 \text{ kDa}$) affinity ligand isolated from pooled normal human serum have been purchased from Sigma-Aldrich. Anti-IgM has been used as capture antibodies as well as detector antibodies. Phosphate buffer saline (PBS) pH 7.2 and ionic strength 163 mM , Tween 20, Sulfosuccinimidyl 4-[N-maleimidomethyl] cyclohexane-1-carboxylate (Sulfo-SMCC), 1 M Tris HCl pH 7.4, NHS-PEG4-Biotin, Streptavidin Horseradish Peroxidase (SA-HRP), Horseradish Peroxidase Substrate- (SuperSignal Luminol), sample diluent (Phosphate buffer with BSA and sodium azide as preservative) were purchased from Quanterix. Universal ELISA plates pre-spotted with an anchor (immobilized protein) were purchased from Quanterix and stored at $2-8 \text{ }^\circ\text{C}$. Anti-IgM capture antibodies against the IgM target proteins were exchanged into phosphate-buffered saline (PBS) and incubated for 30 min at $23 \text{ }^\circ\text{C}$ with Sulfo-SMCC. Maleimide activated capture antibodies were subsequently incubated with a peptide tag purchased from Quanterix used without further purification, at a 1.2 mg mL^{-1} concentration for 30 min at $23 \text{ }^\circ\text{C}$. The maleimide-activated antibody with the peptide occurs through a cysteine group on the peptide. Peptide labeled capture antibodies have been purified via dialysis in PBS using an Amicon Ultra-0.5 Centrifugal Filter Devices. The capture antibodies solution concentration has been adjusted to 0.25 mg mL^{-1} in $1\times$ PBS, 4% BSA, 0.1% sodium azide, and stored at $2-8 \text{ }^\circ\text{C}$ until ready to run the assay. According to standard protocols, anti-IgM detection antibodies were exchanged into PBS and then biotinylated using NHS-PEG4-Biotin ($50\times$ molar excess of biotin to antibody). The biotinylated antibodies were purified from excess biotin by dialysis into PBS using an Amicon filter. IgM calibrator antigen stocks were prepared through serial dilution using the sample diluent.

Assay Development: Anchor antibodies pre-spotted arrays on dried microtiter plates have been washed with $25\times$ Wash Buffer (Tris-based buffer with Tween 20 detergent) on a Simoa washer (Quanterix Corporation) prior to use it. The peptide-tagged anti-IgM capture antibody solution in the sample diluent, with a concentration in the range of $0.1-50 \mu\text{g mL}^{-1}$, with a volume of $50 \mu\text{L}$ has been added to each well of the washed plates. The plates were incubated for 30 min at $23 \text{ }^\circ\text{C}$ while shaken at 525 rpm on an orbital plate shaker. Those shaker parameters have been used for all subsequent incubation steps. When the peptide-labeled anti-IgM capture antibody immobilization has been accomplished, the plates were washed, and a volume of $50 \mu\text{L}$ of IgM calibrator solutions with concentration ranging from 2.5 pg mL^{-1} (2.5 fM , $2.5 \times 10^{-15} \text{ M}$) to 10 ng mL^{-1} (10 pM , 10^{-11} M) has been added into each well. Plates were incubated for 120 min before washing and incubating with $50 \mu\text{L}$ of biotinylated anti-IgM detection antibodies for 30 min . Plates were rewashed, and $50 \mu\text{L}$ of streptavidin-horseradish peroxidase (SA-HRP) enzyme conjugate was added to each well and incubated for 30 min . Finally, the plates were washed before adding $50 \mu\text{L}$ of luminol and hydrogen peroxide to each well. Plates were imaged on the Simoa SP-X (Quanterix Corp.). Fluorescence images were acquired (577 nm excitation and 620 nm emission) and recorded using a CCD camera.^[16]

Experimental Method: A replicated, two-factors, full factorial design has been implemented here. The factors examined were the concentration of anti-IgM capture antibody [CA] and detection antibody [DA], coded with X_1 and X_2 variables, respectively. Following a two-level design, these variables have been set at a low and high level, coded as -1 and $+1$. For each factor, the levels chosen have been 1 and $50 \mu\text{g mL}^{-1}$ for both capture and detection antibodies. The concentration range selected for the capture and detection antibodies is customary to develop ELISA and Simoa SP-X assays.^[19,26,34] The experimental matrix is given in Table 1. The LOD of each assay, computed according to the IUPAC definition,^[35] has been used as the response to the full factorial design. In addition, the LOD at the center point in duplicate has been evaluated and used to validate the linear model with interactions provided by the factorial design. Multilinear

regression has been performed.^[24] The full factorial 2² design and the validation have been performed using CAT (Chemometric Agile Tool) open-source software.^[36]

Acknowledgements

The authors acknowledge Prof. Riccardo Leardi for useful discussions. Academy of Finland projects #316881, #316883, and #332106 “ProSiT—Protein Detection at the Single-Molecule Limit with a Self-powered Organic Transistor for HIV early diagnosis,” Biosensori analitici usa-e getta a base di transistori organici auto-alimentati per la rivelazione di biomarcatori proteomici alla singola molecola per la diagnostica decentrata dell’HIV (6CDD3786), Research for Innovation REFIN—Regione Puglia POR PUGLIA FESR-FSE 2014/2020, PON SISTEMA (MIUR), H2020 – Electronic Smart Systems – SiMBiT: Single-molecule bio-electronic smart system array for clinical testing (Grant agreement ID: 824946), ERCStg 2021 “A binary sensor with single-molecule digit to discriminate biofluids enclosing zero or at least one biomarker” (NoOne) (Proposal ID 101040383), “PMGB – Sviluppo di piattaforme meccatroniche, genomiche e bioinformatiche per l’oncologia di precisione” – ARS01_01195 – PON “RICERCA E INNOVAZIONE” 2014–2020 projects, Åbo Akademi University CoE “Bio-electronic activation of cell functions”, CSGI, are all acknowledged for partial financial support.

Conflict of Interest

The authors declare no conflict of interest.

Data Availability Statement

The data that support the findings of this study are available from the corresponding author upon reasonable request.

Keywords

experimental designs, protein detection, sandwich assays, single molecule arrays, ultrasensitive biosensors

Received: July 27, 2022

Revised: October 1, 2022

Published online: October 28, 2022

- [1] M. Magliulo, A. Mallardi, R. Gristina, F. Ridi, L. Sabbatini, N. Cioffi, G. Palazzo, L. Torsi, *Anal. Chem.* **2013**, *85*, 3849.
- [2] E. Macchia, P. Romele, K. Manoli, M. Ghittorelli, M. Magliulo, Z. M. Kovács-Vajna, F. Torricelli, L. Torsi, *Flexible Printed Electron.* **2018**, *3*, 034002.
- [3] M. Magliulo, D. de Tullio, I. Vikholm-Lundin, W. M. Albers, T. Munter, K. Manoli, G. Palazzo, L. Torsi, *Anal. Bioanal. Chem.* **2016**, *408*, 3943.
- [4] E. Macchia, K. Manoli, B. Holzer, C. di Franco, R. A. Picca, N. Cioffi, G. Scamarcio, G. Palazzo, L. Torsi, *Anal. Bioanal. Chem.* **2019**, *411*, 4899.
- [5] D. A. Giljohann, C. A. Mirkin, *Nature* **2009**, *462*, 461.
- [6] G. S. Ginsburg, S. B. Haga, *Expert Rev. Mol. Diagn.* **2006**, *6*, 179.
- [7] T. R. Golub, D. K. Slonim, P. Tamayo, C. Huard, M. Gaasenbeek, J. P. Mesirov, H. Coller, M. L. Loh, J. R. Downing, M. A. Caligiuri, C. D. Bloomfield, E. S. Lander, *Science* **1999**, *286*, 531.
- [8] M. J. van de Vijver, Y. D. He, L. J. van 't Veer, H. Dai, A. A. M. Hart, D. W. Voskuil, G. J. Schreiber, J. L. Peterse, C. Roberts, M. J. Marton, M. Parrish, D. Atsma, A. Witteveen, A. Glas, L. Delahaye, T. van der Velde, H. Bartelink, S. Rodenhuis, E. T. Rutgers, S. H. Friend, R. Bernards, *N. Engl. J. Med.* **2002**, *347*, 347.
- [9] N. Hu, C. Wang, Y. Hu, H. H. Yang, C. Giffen, Z. Z. Tang, X. Y. Han, A. M. Goldstein, M. R. Emmert-Buck, K. H. Buetow, P. R. Taylor, M. P. Lee, *Cancer Res.* **2005**, *65*, 2542.
- [10] I. Esposito, A. Segler, K. Steiger, G. Klöppel, *Pancreatology* **2015**, *15*, 598.
- [11] J. M. Rothberg, W. Hinz, T. M. Rearick, J. Schultz, W. Mileski, M. Davey, J. H. Leamon, K. Johnson, M. J. Milgrew, M. Edwards, J. Hoon, J. F. Simons, D. Marran, J. W. Myers, J. F. Davidson, A. Branting, J. R. Nobile, B. P. Puc, D. Light, T. A. Clark, M. Huber, J. T. Branciforte, I. B. Stoner, S. E. Cawley, M. Lyons, Y. Fu, N. Homer, M. Sedova, X. Miao, B. Reed, et al., *Nature* **2011**, *475*, 348.
- [12] M. Thompson, S. L. R. Ellison, R. Wood, *Pure Appl. Chem.* **2002**, *74*, 835.
- [13] E. Macchia, K. Manoli, C. di Franco, G. Scamarcio, L. Torsi, *Anal. Bioanal. Chem.* **2020**, *412*, 5005.
- [14] E. Macchia, F. Torricelli, P. Bollella, L. Sarcina, A. Tricase, C. di Franco, R. Österbacka, Z. M. Kovács-Vajna, G. Scamarcio, L. Torsi, *ACS Sensors* **2020**, *5*, 1822.
- [15] D. R. Walt, *Anal. Chem.* **2013**, *85*, 1258.
- [16] D. M. Rissin, C. W. Kan, T. G. Campbell, S. C. Howes, D. R. Fournier, L. Song, T. Piech, P. P. Patel, L. Chang, A. J. Rivnak, E. P. Ferrell, J. D. Randall, G. K. Provuncher, D. R. Walt, D. C. Duffy, *Nat. Biotechnol.* **2010**, *28*, 595.
- [17] C. I. Tobos, S. Kim, D. M. Rissin, J. M. Johnson, S. Douglas, S. Yan, S. Nie, B. Rice, K. J. Sung, H. D. Sikes, D. C. Duffy, *J. Immunol. Methods* **2019**, *474*, 112643.
- [18] M. D. Moody, S. W. van Arsdell, K. P. Murphy, S. F. Orencole, C. Burns, *BioTechniques* **2001**, *31*, 186.
- [19] C. I. Tobos, A. J. Sheehan, D. C. Duffy, D. M. Rissin, *Anal. Chem.* **2020**, *92*, 5613.
- [20] B. Spurrier, P. Honkanen, A. Holway, K. Kumamoto, M. Terashima, S. Takenoshita, G. Wakabayashi, J. Austin, S. Nishizuka, *Biotechnol. Adv.* **2008**, *26*, 361.
- [21] V. Romanov, S. N. Davidoff, A. R. Miles, D. W. Grainger, B. K. Gale, B. D. Brooks, *Analyst* **2014**, *139*, 1303.
- [22] “SP-X Imaging and Analysis System”, can be found under <https://www.quanterix.com/instruments/the-sp-x-imaging-and-analysis-system/>, n.d.
- [23] Sheehan A. I. W. Osmond, R. F. Crouch M, R. Dyer A, *United States Patent 9,086,407*, **2012**.
- [24] M. W. Burke, *Cryst. Growth Des.*, **2001**.
- [25] R. Leardi, *Analytica Chimica Acta* **2009**, *652*.
- [26] G. S. Sittampalam, W. C. Smith, T. W. Miyakawa, D. R. Smith, C. McMorris, *J. Immunol. Methods* **1996**, *190*, 151.
- [27] P. Lems-Van Kan, H. W. Verspaget, A. S. Peña, *J. Immunol. Methods* **1983**, *57*, 51.
- [28] A. Faith, O. Pontesilli, A. Unger, G. S. Panayi, P. Johns, *J. Immunol. Methods* **1982**, *55*, 169.
- [29] E. Macchia, Z. M. Kovács-Vajna, D. Loconsole, L. Sarcina, M. Redolfi, M. Chironna, F. Torricelli, L. Torsi, *Sci. Adv.*, **2022**, *8*, eabo0881.
- [30] L. Sarcina, L. Torsi, R. A. Picca, K. Manoli, E. Macchia, *Sensors* **2020**, *20*, 1.
- [31] D. Copelli, A. Falchi, M. Ghiselli, E. Lutero, R. Osello, D. Riolo, F. Schiaretti, R. Leardi, *Chemom. Intell. Lab. Syst.* **2018**, *178*, 24.
- [32] L. Torsi, M. Magliulo, K. Manoli, G. Palazzo, *Chem. Soc. Rev.* **2013**, *42*, 1.
- [33] E. Macchia, K. Manoli, B. Holzer, C. di Franco, M. Ghittorelli, F. Torricelli, D. Alberga, G. F. Mangiatordi, G. Palazzo, G. Scamarcio, L. Torsi, *Nat. Commun.* **2018**, *9*, 3223.
- [34] D. Wu, M. D. Milutinovic, D. R. Walt, *Analyst* **2015**, *140*, 6277.
- [35] J. Mocak, A. M. Bond, S. Mitchell, G. Scollary, A. M. Bond, *Pure Appl. Chem.* **1997**, *69*, 297.
- [36] “Gruppo di Chemiometria”, can be found under <http://www.gruppochemiometria.it/index.php/software/19-download-the-r-based%20chemometric-software>, n.d.